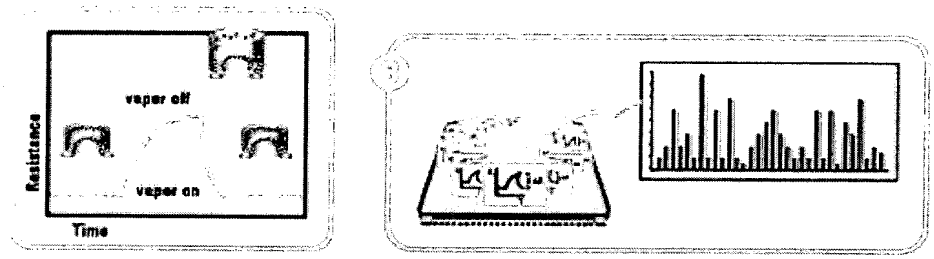

Figure 1. A) A representation of the composite detector material responding during an analyte exposure. B) A representation of how data are converted into response patterns.

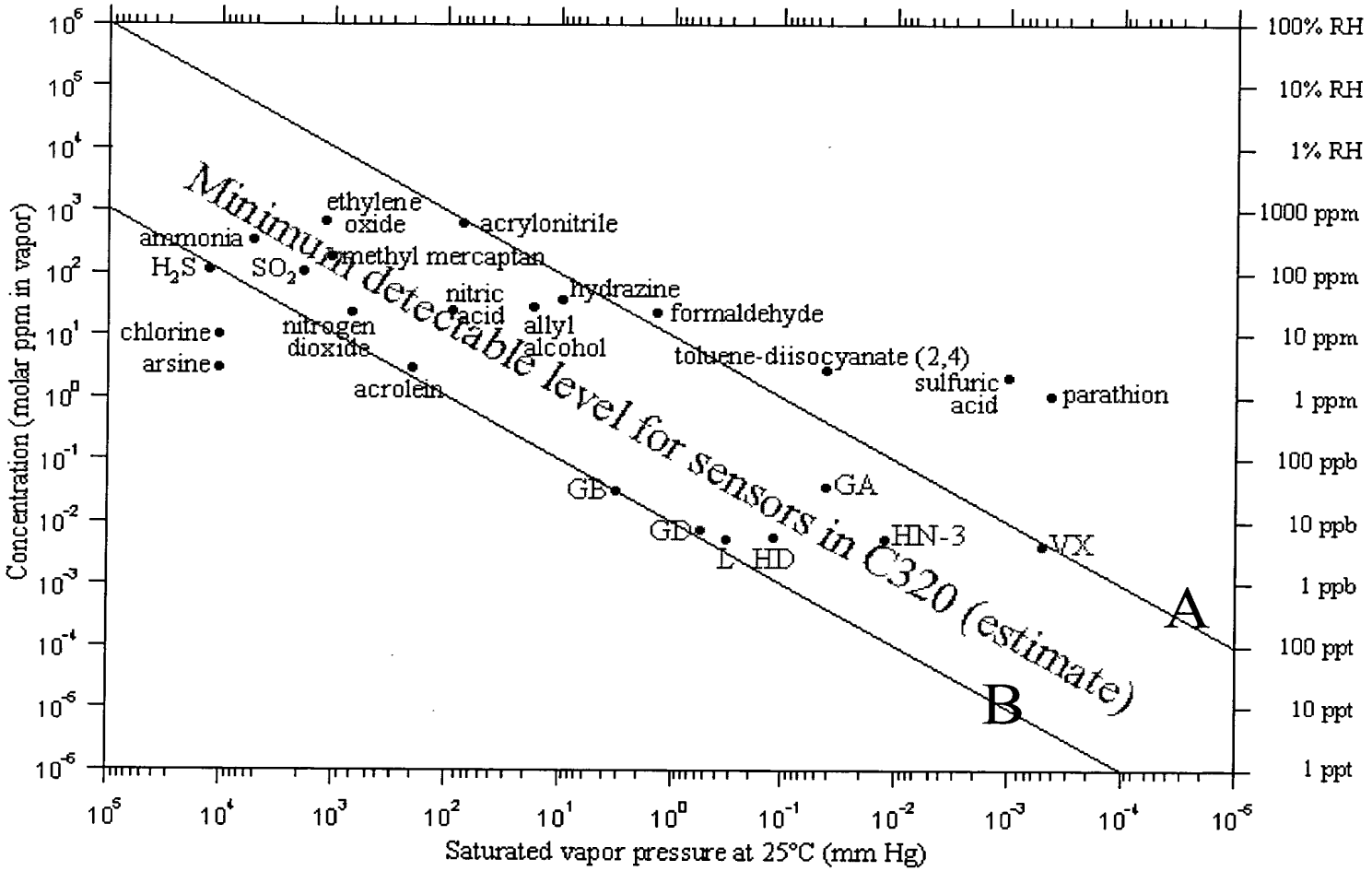

FIG. 2. Points use concentrations of Immediately Dangerous to Life and Health (IDLH) levels. Chemical warfare agents (red) and toxic industrial chemicals (blue) are shown. Chemicals with points above the region for the minimum detectable level have high probability of being detected by the sensor array in the Cyranose 320 at IDLH levels. Chemicals having points within the region have a moderate probability of being detected at IDLH levels. Chemicals having points below the region have a low probability of being detected at IDLH levels.

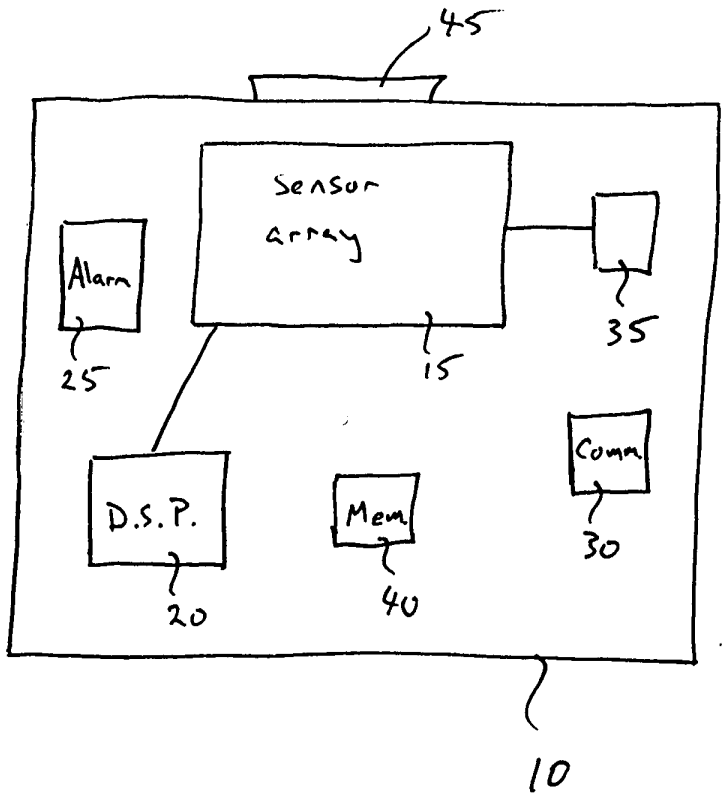

Figure 3a

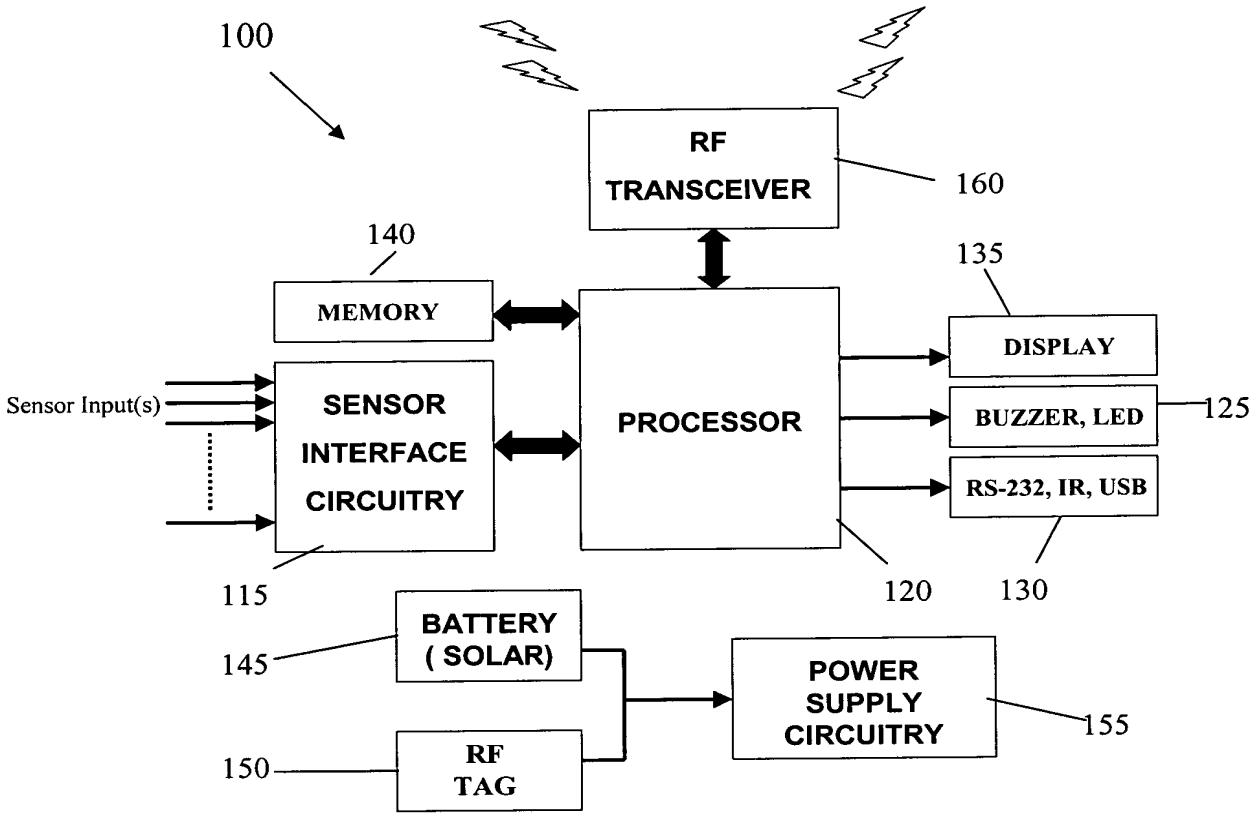
100
RF
TRANSCEIVER
160
140
135
MEMORY
DISPLAY
Sensor Input(s)
SENSOR
INTERFACE
CIRCUITRY
PROCESSOR
BUZZER, LED
125
RS-232, IR, USB
115
120
130
BATTERY
(SOLAR)
145
POWER
SUPPLY
CIRCUITRY
155
150
RF
TAG

FIG.3b

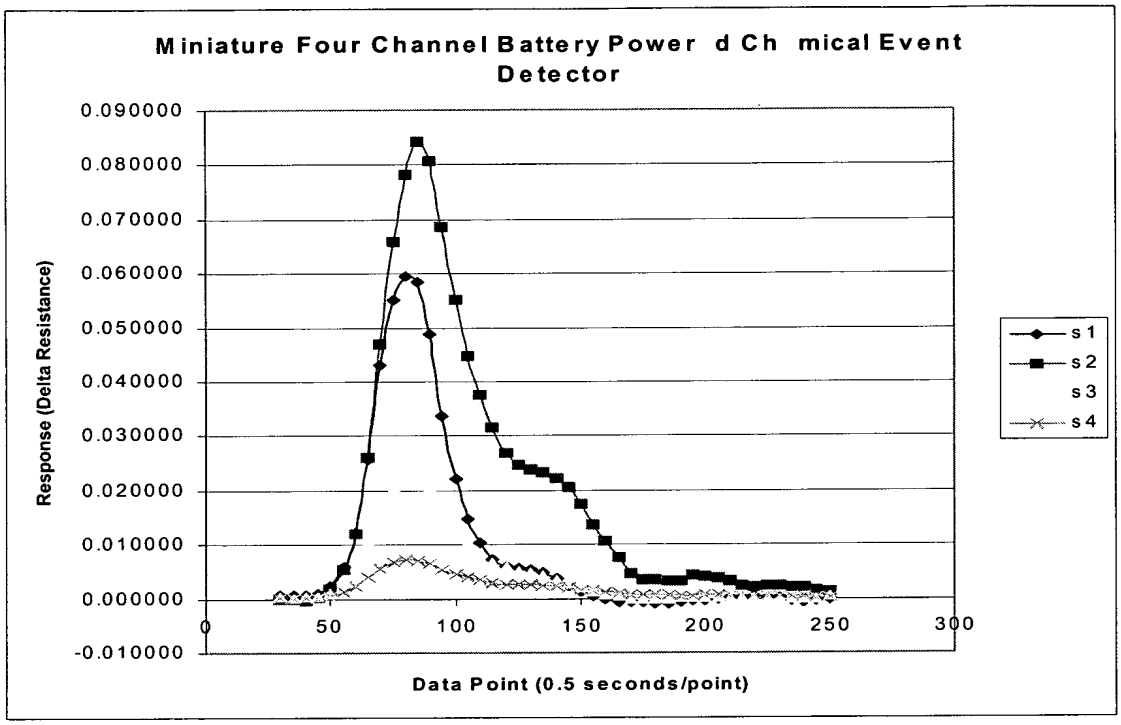

FIG. 4. Typical response curve when a four-channel chemical-event detector is exposed to a transient chemical response.

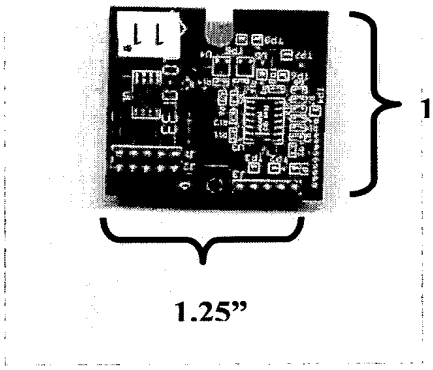

FIG. 5. Four-channel chemical-event detector.

FIG. 6. System architecture for fire detection system. Nodes are defined as a collection of sensors/detectors at a single physical location. Zones are defined by physical relationships between nodes. This multi-level architecture for data analysis makes the system both flexible and scalable.

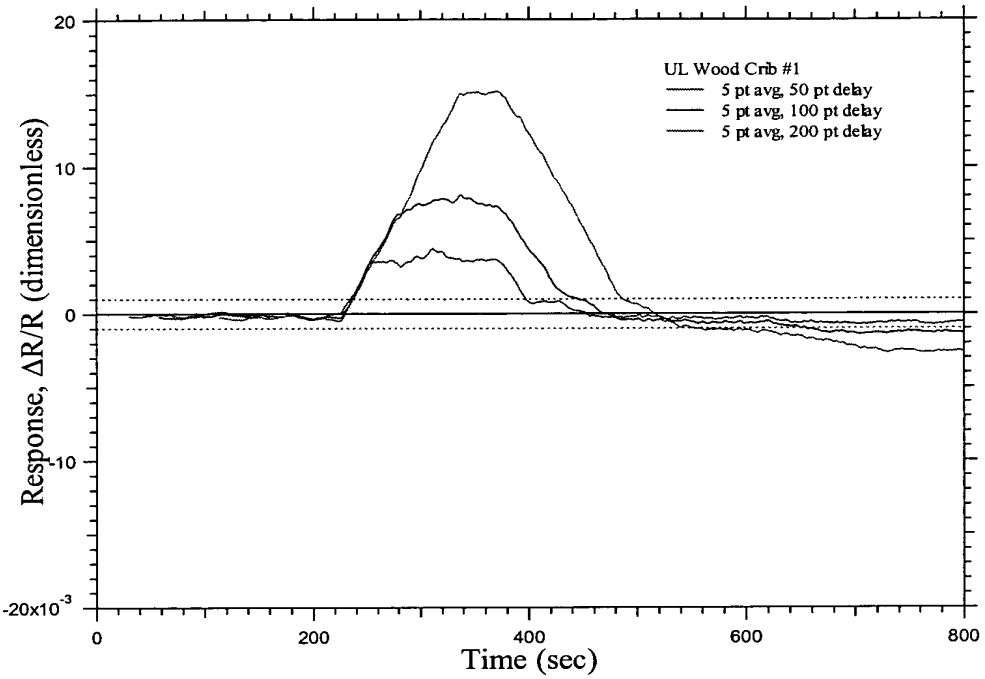

FIG. 7. Response as a function of time for the UL Wood Crib #1 fire. There is a significant difference in the magnitude of the response for different size buffers.

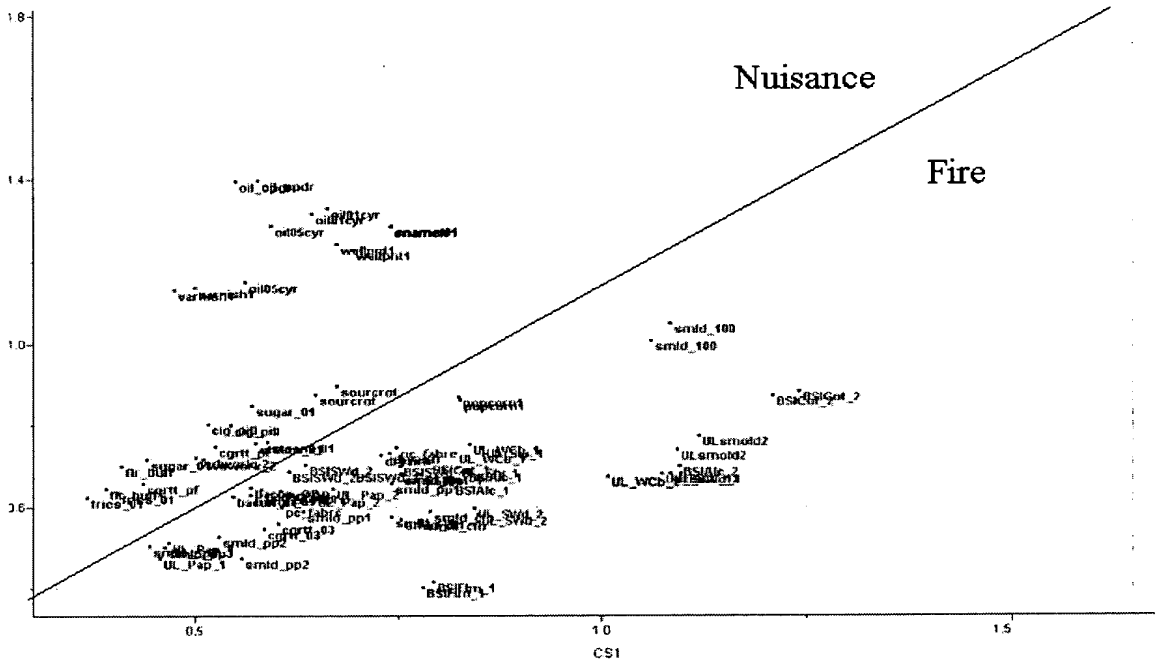

FIG. 8. The results for a Soft Independent Modeling of Class Analogy (SIMCA) model for fire (red) and nuisance tests (blue) that exceed the positive detection threshold. The line separating these two regions was drawn to minimize the number of false negatives---the case where the actual event is a fire but no alarm is sounded.

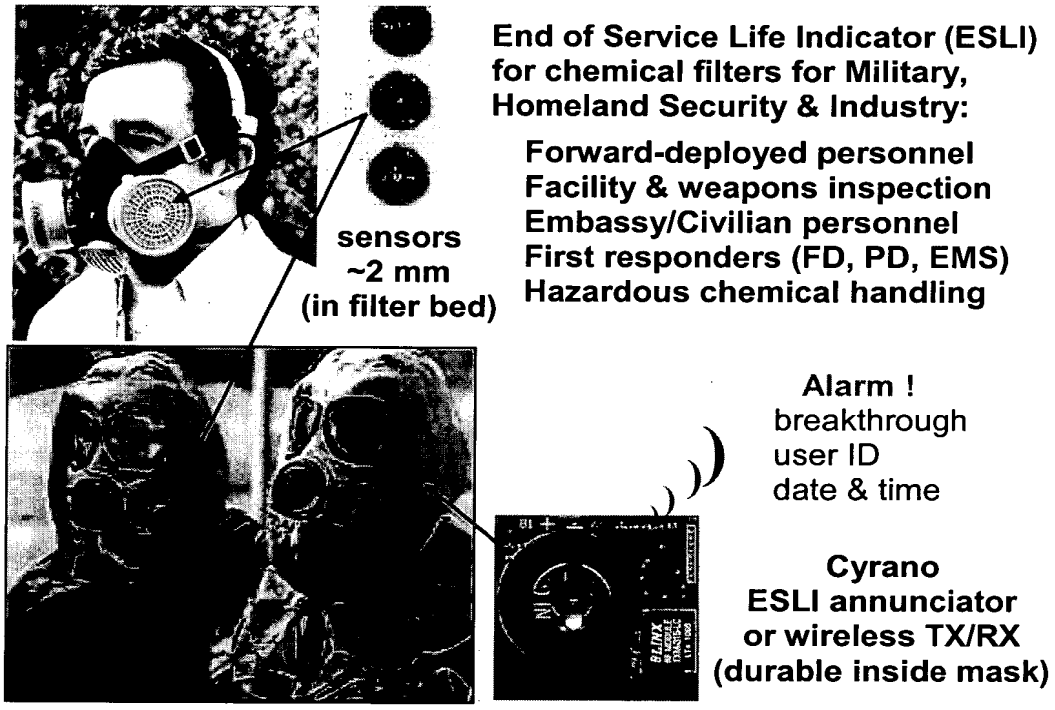

FIG. 9

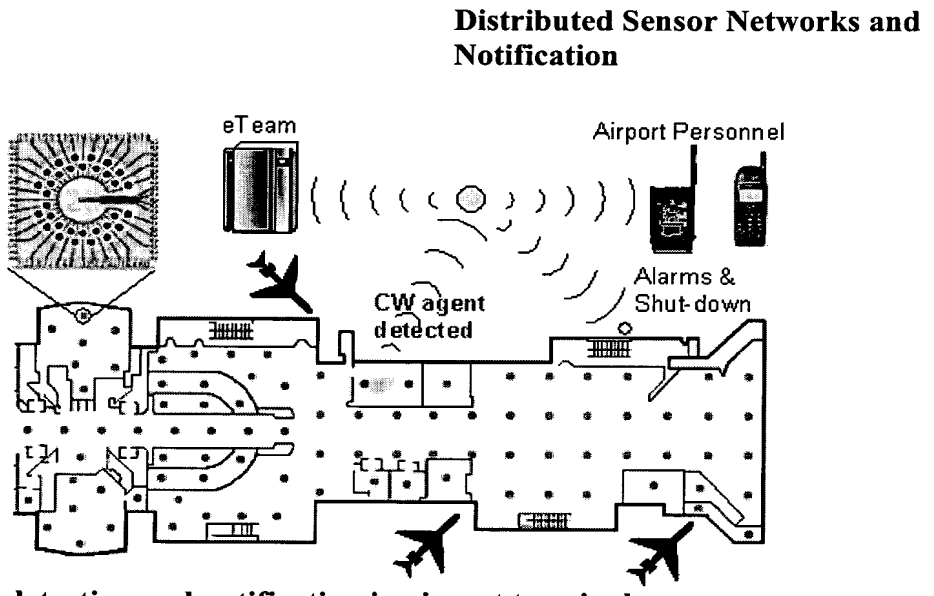

FIG. 10: Remote detection and notification in airport terminals.

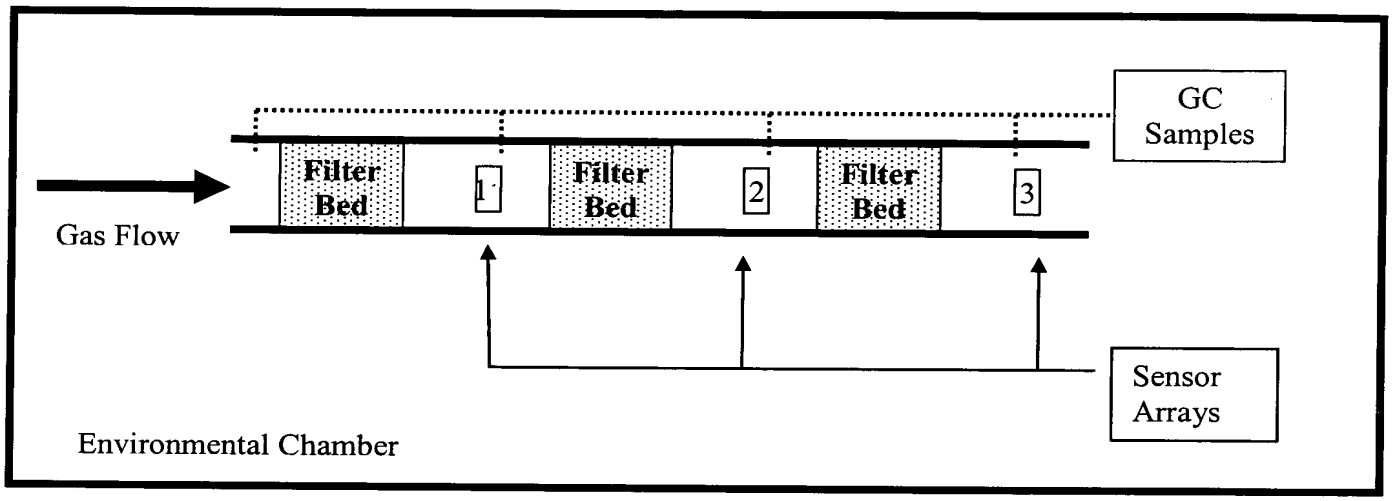

FIG. 11: Schematic Representation of Residual Life Indicator Fixture

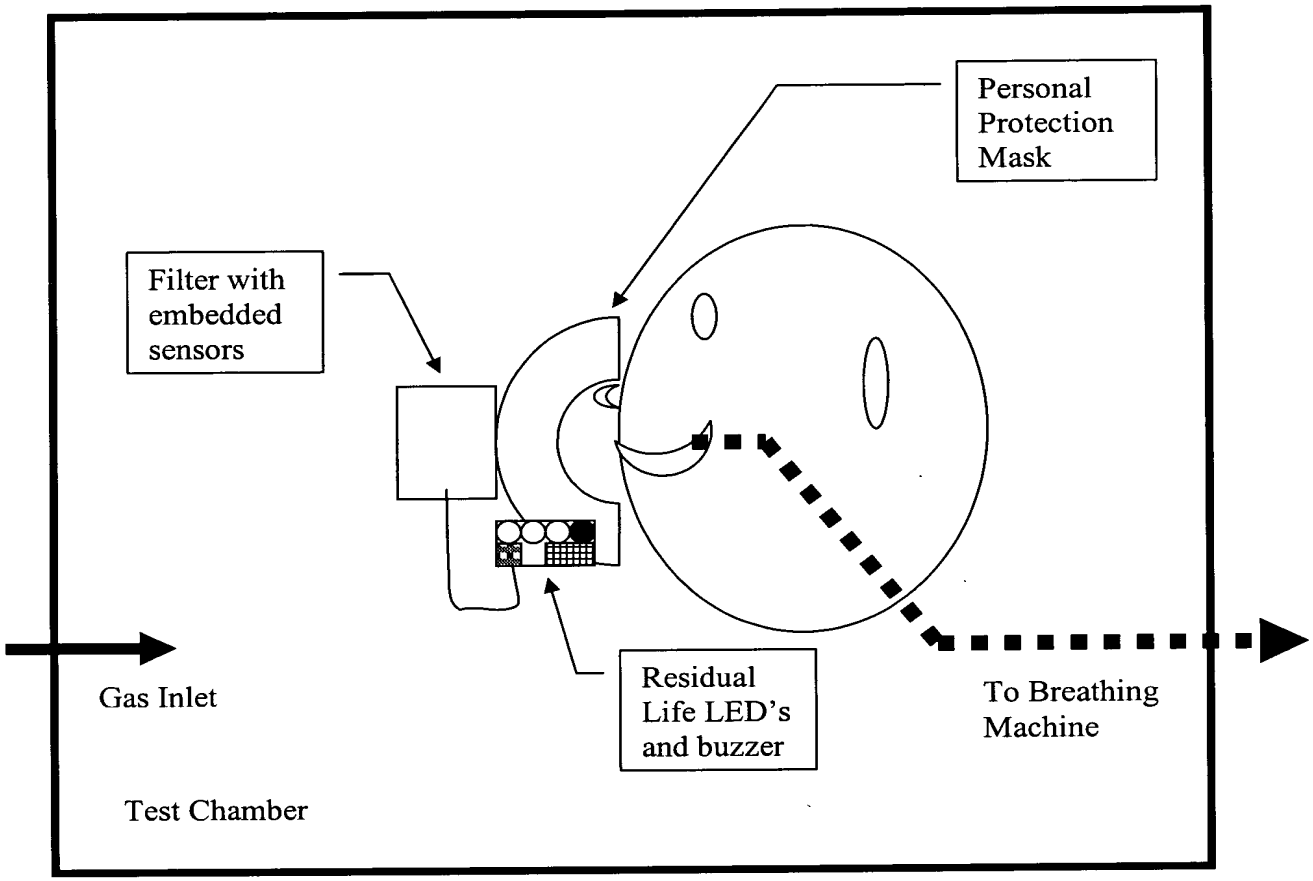
Personal
Protection
Mask
Filter with
embedded
sensors
Gas Inlet
Residual
Life LED's
and buzzer
To Breathing
Machine
Test Chamber

FIG. 12

FIG. 13

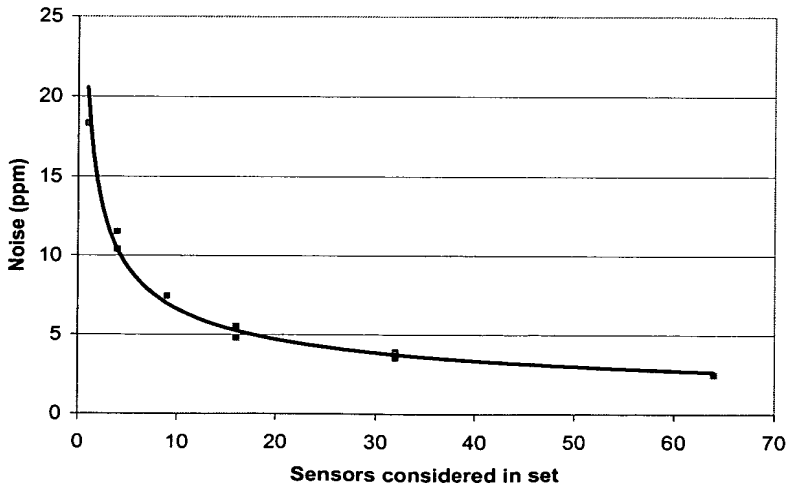
25
20
15
10
5
0
Noise (ppm)
0
10
20
30
40
50
60
70
Sensors considered in set

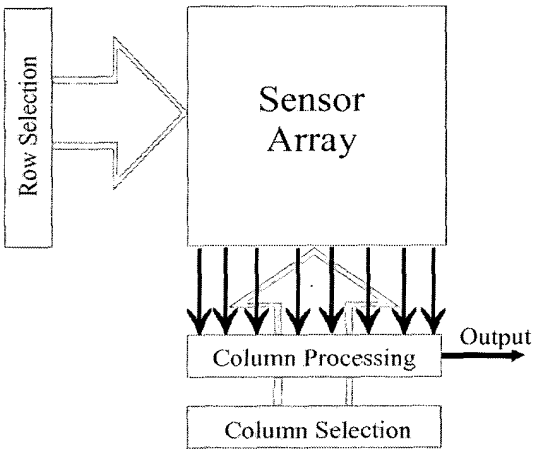
Row Selection
Sensor Array
Output
Column Processing
Column Selection

FIG. 14

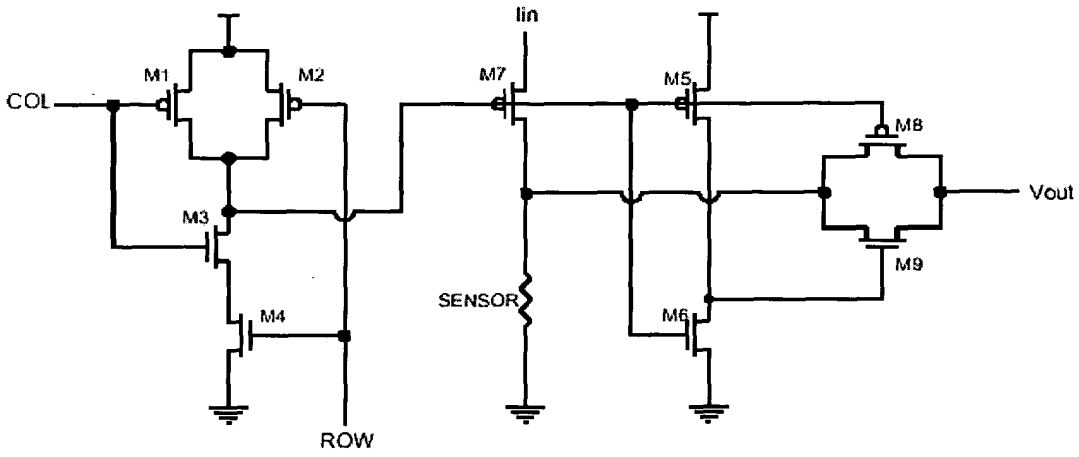
Iin
M1
M2
M7
M5
M8
COL
Vout
M3
M9
SENSOR
M4
M6
ROW

FIG. 15

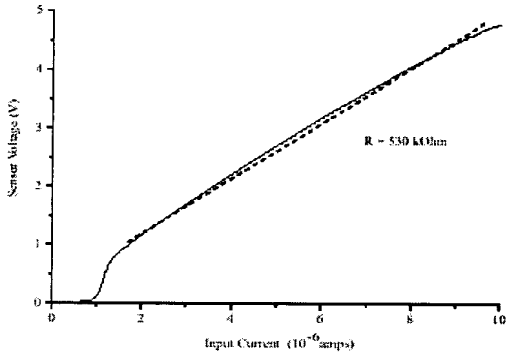
Sensor Voltage (V)
R = 530 kOhm
Input Current (10^{-6} amps)

FIG. 16

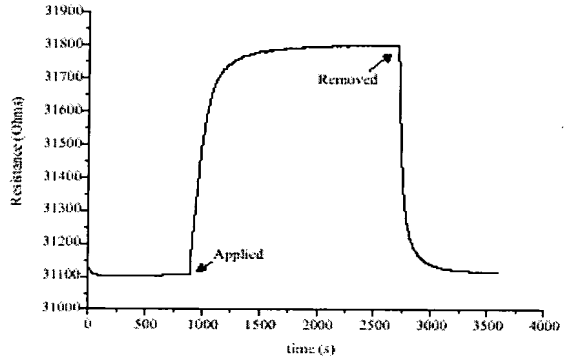
Resistance (Ohms)
Removed
Applied
time (s)

FIG. 17

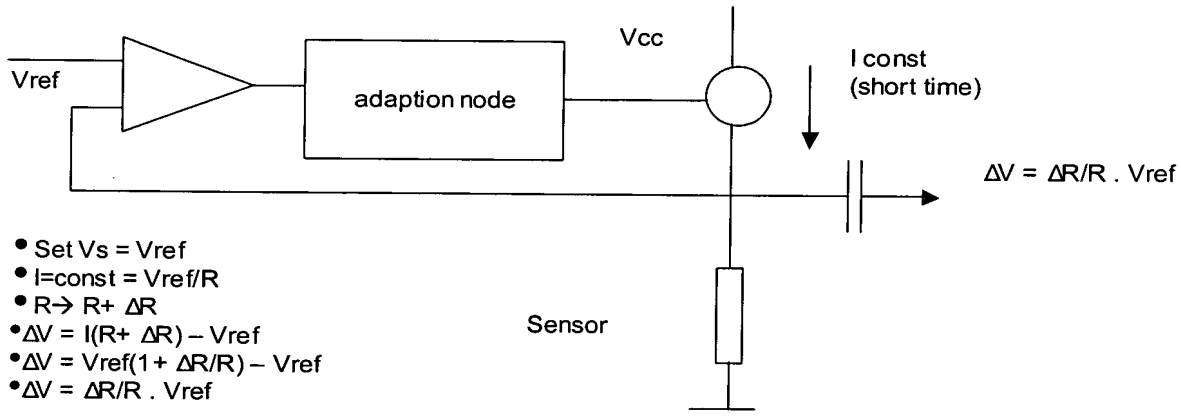
Vref
adaption node
Vcc
I const
(short time)
ΔV = ΔR/R . Vref
Sensor
• Set Vs = Vref
• I=const = Vref/R
• R→ R+ ΔR
•ΔV = I(R+ ΔR) – Vref
•ΔV = Vref(1+ ΔR/R) – Vref
•ΔV = ΔR/R . Vref

FIG. 18

Sample #	Treatment	Solvents	Particle Size nm
6537-57b	Poly(isobutylene) on BP700	Isopar G	150
8847-9a	Polypropylene glycol on BP700	Xylene	180
6537-40	Poly(acrylic ester) on BP700	Ethanol	210
6537-51	Poly(acrylic acid) on BP700	water	210

FIG. 19

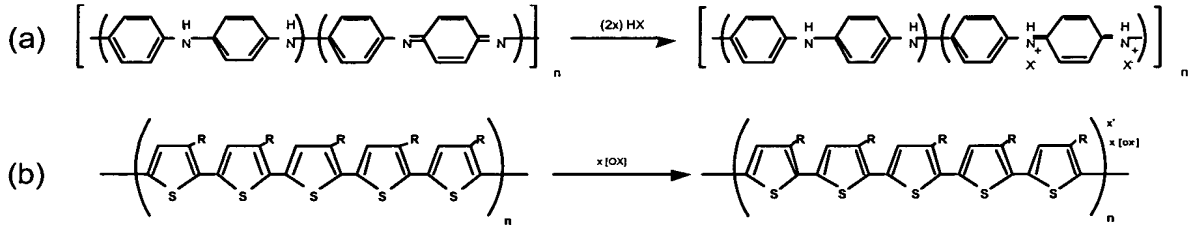

FIG. 20. (a) Chemical structure of polyaniline in its insulating state and its conducting state (following protonation by an acid, HX); (b) chemical structure of poly(3-substituted-thiophene) where R = H, or alkyl, [OX] = oxidizing agent, in its insulating state and its conducting state (following oxidative "doping").

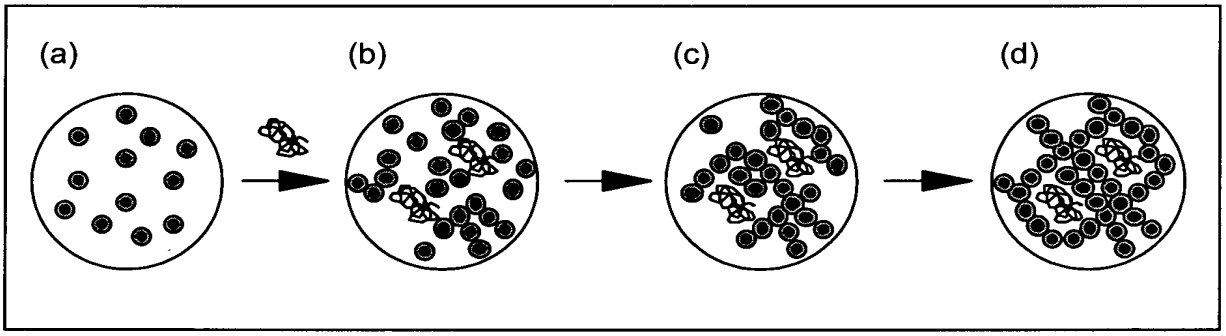

FIG. 21. Schematic diagram of the sol-gel encapsulation of indicator biomolecules. (a) Formation of sol particles during initial hydrolysis and polycondensation. (b) Addition of indicator biomolecule to the sol. (c) The growing silicate network begins to trap the biomolecules. (d) The indicator biomolecules are immobilized in the gel.

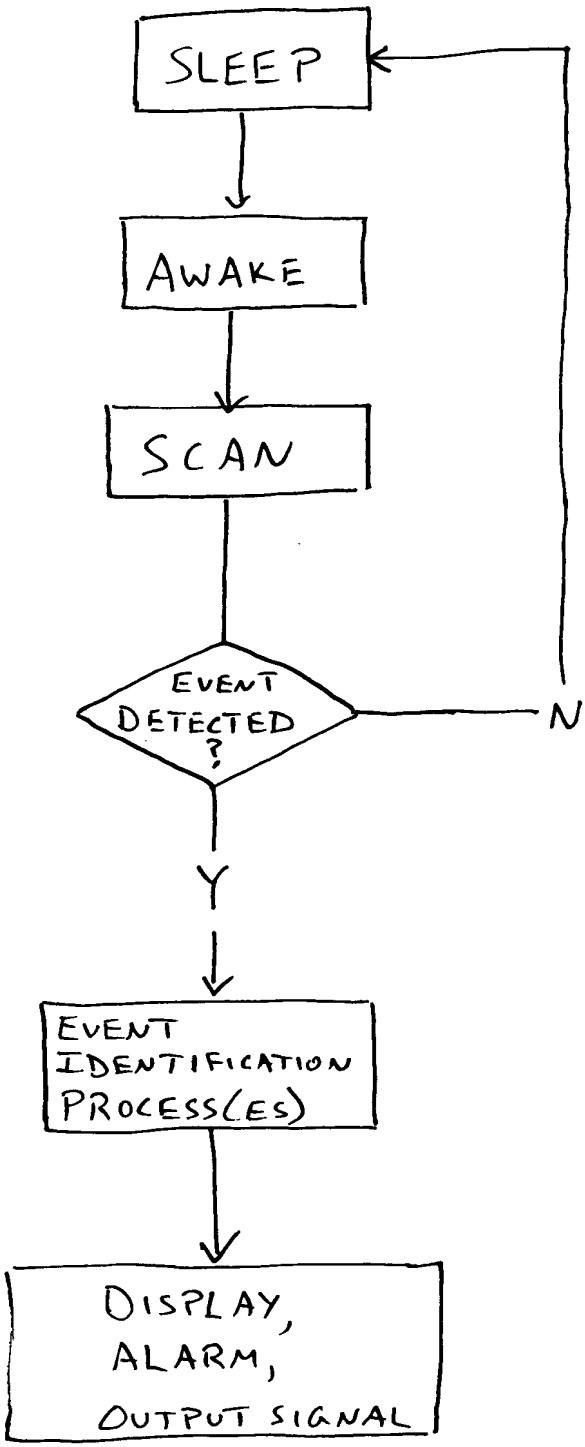
SLEEP
AWAKE
SCAN
EVENT DETECTED ?
N
Y
EVENT IDENTIFICATION PROCESS(ES)
DISPLAY, ALARM, OUTPUT SIGNAL

FIG. 22

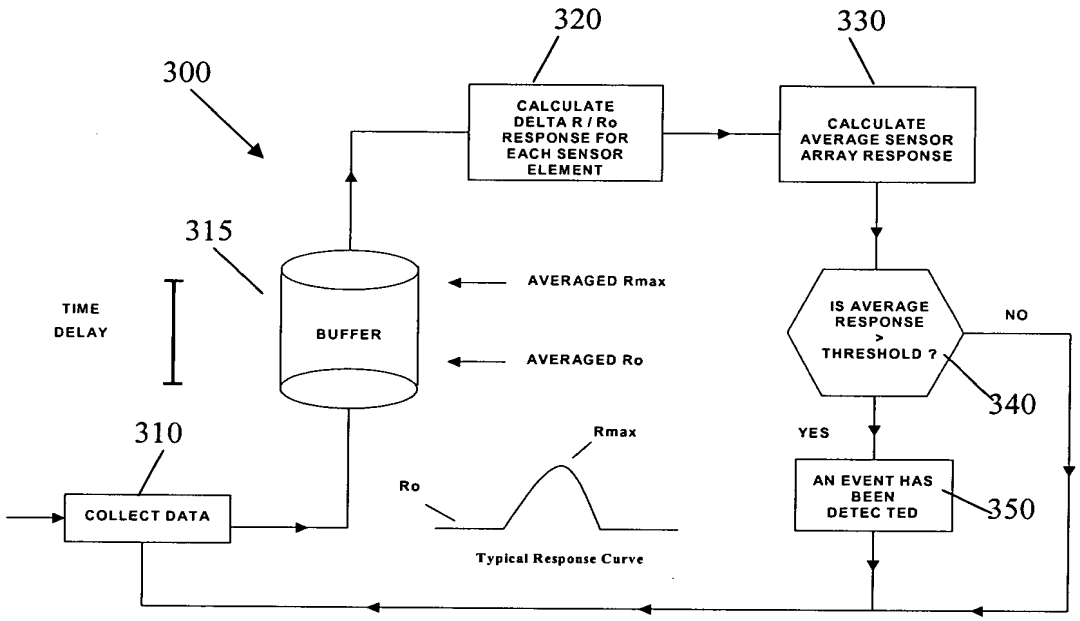

FIG. 23: BLOCK DIAGRAM OF FIRE DETECTION ALGORITHM & TYPICAL SENSOR RESPONSE CURVE